



Dynamic effects of interacting genes underlying rice flowering-time phenotypic plasticity and global adaptation

Tingting Guo, Qi Mu, Jinyu Wang, et al.

Genome Res. published online April 16, 2020

Access the most recent version at doi:[10.1101/gr.255703.119](https://doi.org/10.1101/gr.255703.119)

P<P	Published online April 16, 2020 in advance of the print journal.
Accepted Manuscript	Peer-reviewed and accepted for publication but not copyedited or typeset; accepted manuscript is likely to differ from the final, published version.
Creative Commons License	This article is distributed exclusively by Cold Spring Harbor Laboratory Press for the first six months after the full-issue publication date (see http://genome.cshlp.org/site/misc/terms.xhtml). After six months, it is available under a Creative Commons License (Attribution-NonCommercial 4.0 International), as described at http://creativecommons.org/licenses/by-nc/4.0/ .
Email Alerting Service	Receive free email alerts when new articles cite this article - sign up in the box at the top right corner of the article or click here .

An advertisement banner with a teal background. On the left, the text reads 'CRISPR and RNAi Genetic Screening. Your new superpower.' in white. In the center, there is a white-bordered box containing the words 'LEARN MORE' in teal. On the right, there is a photograph of a woman wearing a red superhero mask and cape, and a green molecular structure logo with the word 'CELLECTA' below it.

CRISPR and RNAi Genetic Screening.
Your new superpower.

LEARN MORE

CELLECTA

To subscribe to *Genome Research* go to:
<https://genome.cshlp.org/subscriptions>

Published by Cold Spring Harbor Laboratory Press

1
2
3 **Dynamic effects of interacting genes underlying rice flowering-time phenotypic plasticity**
4 **and global adaptation**

5
6 Tingting Guo¹, Qi Mu¹, Jinyu Wang¹, Adam Vanous¹, Akio Onogi², Hiroyoshi Iwata³, Xianran Li^{1,*}, and Jianming
7 Yu^{1,*}

8
9 ¹Department of Agronomy, Iowa State University, Ames, IA 50011, USA

10 ²Institute of Crop Science, National Agriculture and Food Research Organization, Ibaraki 305-8518, Japan

11 ³Department of Agricultural and Environmental Biology, University of Tokyo, Tokyo 113-8657, Japan

12 *Corresponding authors. Emails: jmyu@iastate.edu; lixr@iastate.edu

13
14 **Keywords:** phenotypic plasticity, flowering time, genotype by environment interaction, reaction norm,
15 genomics, haplotype, adaptation

16
17 **Abstract**

18 Phenotypic variation of living organisms is shaped by genetics, environment, and their
19 interaction. Understanding phenotypic plasticity under natural conditions is hindered by the
20 apparently complex environment and the interacting genes and pathways. Herein, we report
21 findings from the dissection of rice flowering-time plasticity in a genetic mapping population
22 grown in natural long-day field environments. Genetic loci harboring four genes originally
23 discovered for their photoperiodic effects (*Hd1*, *Hd2*, *Hd5*, and *Hd6*) were found to differentially
24 respond to temperature at the early growth stage to jointly determine flowering time. The effects
25 of these plasticity genes were revealed with multiple reaction norms along the temperature
26 gradient. Coupling genomics and the environmental index, accurate performance predictions
27 were obtained. Next, we examined the allelic variation in the four flowering-time genes across
28 the diverse accessions from the 3,000 Rice Genomes Project, and constructed haplotypes at both
29 individual-gene and multi-gene levels. The geographic distribution of haplotypes revealed their
30 preferential adaptation to different temperature zones. Regions with lower temperature were
31 dominated by haplotypes sensitive to temperature changes, while the equatorial region had a
32 majority of haplotypes that are less responsive to temperature. Integrating knowledge from
33 genomics, gene cloning and functional characterization, and environment quantification, we
34 proposed a conceptual model with multiple levels of reaction norms to help bridge the gaps
35 among individual gene discovery, field-level phenotypic plasticity, and genomic diversity and
36 adaptation.

37

38 Introduction

39 Understanding the genetic and environmental mechanisms of phenotypic plasticity has been a
40 long-term challenge (Marais et al. 2013; Josephs 2018). Advances in genomics and molecular
41 biology allowed further exploration of the genetic architecture of complex traits under natural
42 field conditions (Marais et al. 2013; Blackman 2017; Li et al. 2018; Millet et al. 2019). Rice
43 (*Oryza sativa* L), with a large number of genes cloned for agronomic traits, is well-positioned to
44 bridge the gap among genomic diversity, individual genes, and field-level phenotypic plasticity
45 dissection (Nicotra et al. 2010; Chen et al. 2019). Rice accounts for about one-fifth of the
46 world's caloric intake. Population growth drives up the global demand for food that is expected
47 to increase for the next several decades (Godfray et al. 2010). Producing more rice from less
48 arable land under fluctuating climatic conditions requires a concerted effort from both public and
49 private sectors. Although advances in genomics, breeding, and precision agriculture have been
50 recognized as solution components for global food security (McCouch et al. 2013; Huang et al.
51 2015; Zeng et al. 2017; Wang et al. 2018), enriched knowledge of the varied performance of
52 genotypes across environments, or phenotypic plasticity (Nicotra et al. 2010), is required to
53 design and implement the best genetic deployment and agronomic management practices.

54
55 Flowering time plays a critical role in rice adaptation and production, and modification of
56 flowering time is determined by genetic pathways that integrate endogenous and exogenous
57 signals (Hori et al. 2016). The worldwide distribution of rice is the manifestation of the large
58 genetic diversity adapted to varying environmental conditions (Wang et al. 2018). Because
59 flowering time also affects other agronomic traits, genetic improvement in rice often involves the
60 selection of flowering time for yield optimization.

61
62 Molecular mechanisms underlying the timing of transition from vegetative to reproductive
63 growth have been extensively studied in rice (Xue et al. 2008b; Huang et al. 2012b; Yano et al.
64 2016), a model crop species. *Heading date 1* (*Hd1*), a homolog of *CONSTANS* from *Arabidopsis*,
65 is a central regulator of flowering time in rice, a facultative short day-length (SD) plant (Yano et
66 al. 2000). *Hd1* promotes *Heading date 3a* (*Hd3a*, a florigen-coding gene) expression in SD and
67 suppresses the expression of *Hd3a* in long day-length (LD) conditions (Hayama et al. 2003;
68 Tamaki et al. 2007; Nuñez and Yamada 2017). *OsGIGANTEA* (*OsGI*) acts as an activator of *Hd1*
69 under SD. In addition to the *OsGI-Hd1-Hd3a* photoperiodic pathway branch, a second branch,
70 *Ghd7-Ehd1-RFT1*, also affects rice flowering time (Hayama et al. 2003; Shrestha et al. 2014;
71 Zhang et al. 2017). *Ehd1* promotes flowering by activating the expression of *Hd3a* and *RFT1*
72 (another florigen-coding gene). *Ghd7* acts as a LD-preferential repressor by blocking the
73 expression of *Ehd1* (Xue et al. 2008a). *Hd2* and *Hd5* are key regulators in the *Ehd1* pathway,
74 while *Hd6* plays a critical role in regulating *Hd1* activity (Takahashi et al. 2001; Wei et al. 2010;
75 Koo et al. 2013). In addition, as in *Arabidopsis*, flowering in rice is induced by the coincidence
76 of circadian and solar rhythms for *Hd1* and *Ehd1*, consistent with the external coincidence model
77 (Yeang 2013).

78
79 Although natural variants of these genes were associated with flowering time in diverse rice
80 accessions (Zhao et al. 2011; Huang et al. 2012b; Yano et al. 2016), integration of these findings
81 to explain and predict complex phenotypic plasticity observed in natural fields has received
82 limited attention. A recent review highlighted the research need to examine gene-environmental
83 interaction and gene-gene interaction (Chen et al. 2019). An earlier study examined the

84 flowering-time plasticity in a sorghum bi-parental population (Li et al. 2018), but how findings
85 from a narrow genetic background can be connected with diverse germplasm remains unclear.
86 Herein, we show that the key flowering-time genes (*Hd1*, *Hd2*, *Hd5*, and *Hd6*), originally
87 discovered for their photoperiodic responses, are the major loci responding to the varied
88 temperature at nine different environments for a genetic mapping population. Their dynamic
89 effects and interactions shape the complex phenotypic-plasticity landscape. Reaction norms of
90 gene effects can be obtained along the temperature gradient differentiating these environments.
91 Moving into a broader genetic context, we constructed the multi-gene haplotypes for the diverse
92 accessions from the 3,000 Rice Genomes Project. Leveraging the known functional
93 polymorphisms of these well-studied genes, we assigned the slope parameter values obtained
94 from the bi-parental population to these haplotypes. A clear preferential distribution pattern
95 emerged for haplotypes with different sensitivity to temperature zones. Finally, we proposed a
96 conceptual model to illustrate phenotypic complexity using the multiple levels of reaction norms
97 along an environmental gradient.

98

99 **Results**

100 **Rice flowering-time plasticity in natural long-day environments**

101 Complex flowering time (heading date) variation was observed in a rice genetic mapping
102 population grown in nine natural environments (**Fig. 1A,B; Supplemental Table S1**). This
103 population is a group of 174 backcross inbred lines derived from crossing two parents. One
104 parent is a *japonica* cultivar, Koshihikari, and the other parent is an *indica* cultivar, Kasalath.
105 The latitudes of field sites range from 21°01'N (Vietnam) to 36°01'N (Japan), while planting
106 time ranged from March to June. Environmental mean, the average flowering time of the whole
107 population within each environment, varied from 68 to 121 days after planting (DAP). Trait
108 correlation and prediction of flowering time for each pair of environments ranged from 0.20 to
109 0.99 and 0.17 to 0.91, respectively (**Supplemental Fig. S1**). Flowering time expressed as DAP
110 exhibited a pattern that can be readily modeled, unlike using growing-degree-days (GDD) as the
111 flowering-time unit (**Supplemental Fig. S2**).

112

113 We first conducted several analyses to understand the overall phenotypic variation and genotype
114 by environment interaction ($G \times E$) (Malosetti et al. 2013). Variance component analysis
115 partitioned the phenotypic variance into environment (73.3%), genotype (17.6%), and $G \times E$
116 (8.9%) (**Supplemental Tables S2-S3**). We then partitioned the $G \times E$ variance into lack of
117 genetic correlation (79.0%) and heterogeneity of genotypic variance (21.0%) (**Supplemental**
118 **Table S4**). Following the additive main effects and multiplicative interaction (AMMI) model, we
119 found that the first two principal components accounted for 82.3% of the $G \times E$ (**Fig. 1C**). With
120 the joint regression analysis approach (Finlay and Wilkinson 1963; Eberhart and Russell 1966),
121 $G \times E$ was partitioned into heterogeneity in slopes (73.3%) and error (26.7%) (**Supplemental**
122 **Table S5**).

123

124 We focused our attention on joint regression analysis, which models the overall phenotypic
125 variation with a numerical index (environmental mean) to connect all environments (**Fig. 1D**).
126 By regressing the observations of individual genotypes on environmental mean, one can obtain
127 the expected reaction norm of this genetic population. Despite two parents exhibiting relatively
128 small differences, their progenies showed transgressive segregation in flowering time (**Fig. 1D**).
129 Although grouping patterns emerged in both genotypes and environments, this traditional joint

130 regression analysis relies on environmental mean and could not discern the underlying biological
131 mechanisms or allow performance prediction of other environments.

132

133 **Temperature defines the environmental index capturing flowering-time variation**

134 A better understanding of the general environmental pattern is needed to facilitate both
135 systematic gene effect comparison and performance prediction. As an aggregate measure,
136 environmental mean represents the outcome of the interplay between genetics and environment.
137 If we regard the whole population as a single genotype, environmental mean informs us about
138 differences among environments. However, environmental mean can only be obtained after the
139 actual experiment and is specific to the tested set of environments, lacking the capability of
140 inference.

141

142 We examined ways to replace environmental mean by an explicit, performance-derived
143 environmental index (**Supplemental Table S6**). After testing temperature (using growing degree
144 days, GDD), photoperiod, and photothermal time (PTT) from different growth windows
145 (**Supplemental Fig. S3**), we found that average temperature from 9-50 DAP (denoted as GDD_{9-50})
146 can serve as an environmental index to best characterize the environments and replace
147 environmental mean (**Fig. 2A,B**). Besides having a strong correlation ($r = -0.990$, $P = 3 \times 10^{-7}$)
148 (**Fig. 2C**), GDD_{9-50} involves a biologically relevant window covering the early growth stage
149 when plants process the environmental cues to determine the timing of transition to reproductive
150 development. All nine environments were regarded as LD environments because the average
151 daily photoperiod before flowering ranged from 13.9 to 15.5 hours (**Supplemental Fig. S4**),
152 greater than 13.5-hour threshold for the general SD and LD classification (Itoh et al. 2010).
153 Correlation between photoperiod and environmental mean was only 0.38 in the same 9-50 DAP
154 window (**Supplemental Fig. S3**). Due to the negligible increase in correlation strength when
155 considering photoperiod as an additional environmental factor to pair with temperature, PTT ($r =$
156 -0.991) was not chosen (**Supplemental Fig. S3**). In addition, subsampling analyses verified the
157 general consistency of this GDD_{9-50} across both subsets of environments and subsets of
158 genotypes (**Supplemental Fig. S5**).

159

160 With the identified environmental index, the fitted reaction norm of this genetic population was
161 obtained by regressing flowering-time observations from each genotype on the values of GDD_{9-50}
162 (**Fig. 2D**). The varied responses among individual genotypes can be described by two reaction-
163 norm parameters: 1) intercept, quantifying the overall expected flowering time, and 2) slope,
164 quantifying the sensitivity to environmental changes. One-unit increase in temperature promoted
165 the whole population to flower 1.94 days earlier, while this value varied between 0.6 to 3.6 days
166 for different genotypes (*i.e.*, different slopes).

167

168 **Performance prediction through joint genomic regression analysis (JGRA)**

169 To first focus on the whole-plant performance level, we implemented JGRA to model and
170 predict flowering time for this rice population by integrating the identified environmental index,
171 joint regression analysis, and genomic selection. With the whole population being genotyped, we
172 tested two approaches: 1) genomic predicted reaction-norm parameters for individual genotypes
173 (**Fig. 3A-C**) and 2) genome-wide marker effect continua for individual markers (**Fig. 3D-F**). All
174 162 markers across the genome were used to construct the genomic relationship matrix for
175 reaction norm parameters or derive the genome-wide marker effects. Although this marker

176 number appeared small, it is known that the requirement for the number of markers in bi-parental
177 population is generally low (Bernardo and Yu 2007). We examined three scenarios by splitting
178 environments and genotypes into either tested or untested.

179
180 High prediction accuracy (*i.e.*, correlation between predicted and observed values) was obtained
181 from both JGRA approaches for predicting performance of tested genotypes in untested
182 environments (leave-one-environment-out cross-validation): 0.97 and 0.94 (**Fig. 3A,D**).
183 Prediction accuracy within individual environment varied from 0.82 to 0.99 for the reaction-
184 norm parameter approach and from 0.71 to 0.90 for the marker effect continuum approach. The
185 predicted values were very close to the observed values, with a ratio close to 1 (**Supplemental**
186 **Fig. S6**). For the second scenario, predicting the performance of untested genotypes in tested
187 environments (leave-one-half-genotypes-out cross-validation), prediction accuracy was 0.91 and
188 0.89 (**Fig. 3B,E**). This scenario describes when only a proportion of possible genotypes can be
189 tested in different environments due to either limited resources or by design and predictions of
190 the remaining untested genotypes are made. Prediction accuracy within individual environment
191 ranged from 0.45-0.66 and 0.46-0.67 for the two approaches, lower than the first scenario. The
192 ratio of predicted values to observed values were close to 1 on average in the second scenario
193 (**Supplemental Fig. S6**).

194
195 For the most challenging scenario, predictions for untested genotypes in untested environments,
196 connecting tested and untested genotypes with genome-wide markers and connecting tested and
197 untested environments with environmental index were needed (**Fig. 3C,F**). The leave-one-
198 environment-and-one-half-genotypes-out cross-validation resulted in an accuracy of 0.88 for the
199 reaction-norm parameter approach and 0.90 for the marker effect continuum approach, and
200 individual-environment accuracy of 0.44-0.67. We further demonstrated that in all three
201 scenarios, the series of environment-specific predictions generated from JGRA were superior to
202 the fixed predictions using average performance across tested environments (best linear unbiased
203 estimator, BLUE) (**Supplemental Fig. S6**).

204
205 Prediction accuracy across all environments was higher than those for individual environments.
206 This was expected given the wider context for the across-all-environments prediction (*i.e.*, range
207 change for x - y correlation of *predicted-observed*) and that across-all-environments correlation
208 contains the environment effect that was well captured by the environmental index. Biologically,
209 unique local environmental conditions may alter flowering time in different directions from the
210 main environmental factor across environments and thus reduce prediction accuracy.

211
212 Following the framework of joint regression analysis (Finlay and Wilkinson 1963; Eberhart and
213 Russell 1966), we partitioned the overall variance in the predicted values into components
214 (**Supplemental Table S7**). As expected, contribution of environment to phenotypic variance was
215 the highest, followed by genotype and $G \times E$.

216 217 **Genetic dissection of flowering-time plasticity**

218 To reveal the underlying genetic loci and their effect dynamics, we conducted QTL linkage
219 mapping using flowering-time observations within individual environments, mapping using
220 flowering-time observations across environments, and mapping using two reaction-norm
221 parameters (intercept and slope). Although the environment effect accounted for a large part of

222 the overall phenotypic variation in the multi-environment trial (73.3%), genotypic variance was
223 twice of genotype by environment variance and entry-mean based heritability of flowering time
224 was 0.946 (**Supplemental Tables S2-S4**). The detection of QTLs was not affected because the
225 heritability for single environment was moderately high (0.662). Consistently, four loci
226 corresponding to *Hd1*, *Hd2*, *Hd5*, and *Hd6* were detected by all mapping approaches (**Fig. 4A,B**;
227 **Supplemental Fig. S7-S8**).

228
229 Given the well-studied photoperiod response in rice (Matsubara et al. 2014) and available
230 genome sequence information of two parental inbreds (Wang et al. 2018), we verified the
231 functional polymorphisms in these four genes (*Hd1*, *Hd2*, *Hd5*, and *Hd6*) (**Fig. 4C**;
232 **Supplemental Fig. S9**; **Supplemental Table S8**). In addition, all four genes were originally
233 identified by map-based cloning involving Kasalath, one of the mapping parents and Nipponbare,
234 the reference genome. All this information allowed us to connect these four cloned genes with
235 the mapped QTLs. We adapted the known pathway (Matsubara et al. 2014) to show their
236 additional roles for temperature sensing to control flowering time (**Fig. 4D**). The effect of
237 temperature on flowering time and through genes identified from the photoperiodic response
238 pathway were documented in the earlier studies (Vergara and Chang 1985; Li et al. 2015b). In
239 the current study, the Koshihikari allele of *Hd1* delayed flowering in most of the environments,
240 which agrees with the function of *Hd1* as a repressor of *Hd3a* in LD condition, and the effect
241 was dependent on the temperature. Comparing with the *Hd2* allele from Kasalath, *Hd2* allele
242 from Koshihikari promoted flowering in environments with GDD₉₋₅₀ greater than 20, while
243 repressing flowering in environments with GDD₉₋₅₀ less than 20. The negative genetic effects of
244 *Hd5* and *Hd6* indicated that Koshihikari alleles promoted flowering across the temperature range
245 captured in these tested environments.

246
247 Having the same set of loci detected from mapping using flowering-time observations (**Fig. 4A**)
248 and mapping using reaction-norm parameters (**Fig. 4B**) indicated these plasticity genes were
249 responding to the temperature gradient that differentiated the environments (Nicotra et al. 2010).
250 In addition, different orders of QTL effects were identified: *Hd5*, *Hd1*, *Hd6*, and *Hd2* for
251 intercept, but *Hd1*, *Hd2*, *Hd5*, and *Hd6* for slope (**Fig. 4B**), which agreed with reaction norms of
252 genetic effects at single-locus level along the environmental index defined by temperature (**Fig.**
253 **4A**). Using effect estimates (**Fig. 4B**) from mapping with reaction-norm parameters (**Fig. 2D**),
254 reaction norms of genetic effects for four loci can also be plotted, which is comparable to the plot
255 from mapping first and regression next (**Fig. 4A**). Reaction norms at different resolution levels
256 showed consistent patterns (**Supplemental Methods**; **Supplemental Fig. S10-S12**).

257
258 To examine contributions from additive effect and QTL by environment interaction (QEI) effect,
259 we conducted QEI mapping (Li et al. 2015a) (**Supplemental Fig. S8**). Agreement was found
260 between the results from QTL mapping with intercept and slope. *Hd1*, *Hd5*, and *Hd6* were
261 detected mainly by additive effect, while *Hd1* and *Hd2* were detected mainly by QEI effect. *Hd2*
262 was the most significant gene controlling QEI as the effect of *Hd2* is bidirectional, promoting or
263 repressing flowering depending on the environment it was exposed to. To discover the
264 interaction between genes, we carried out QEI mapping on epistasis and detected strong
265 interaction signals between *Hd2* and *Hd6*, and between *Hd1* and *Hd5* (**Supplemental Fig. S8**).
266 Additionally, other signals with intermediate strength across the genome were detected,
267 indicating that many small-effect interactions also contributed to the flowering-time variation. It

268 appears that even though complex pathways and networks might have been involved, strong
269 marginal effects and two-way interactions can still be detected.

270

271 Alternative to genomic prediction using genome-wide markers, flowering time can also be
272 predicted by constructing a model with only markers tagging these four genes (**Supplemental**
273 **Fig. S13**). Comparable results were obtained, which is expected given the common framework of
274 environmental index search and joint regression analysis.

275

276 **Haplotype networks of four flowering-time plasticity genes in global germplasm**

277 It is interesting to see how different alleles and allele combinations are present in diverse rice
278 accessions. This is because we observed the differential temperature responses of these four
279 genes originally discovered from their photoperiod effects and a recent genome scan with whole-
280 genome sequencing identified *Hd1*, *Hd2*, and *Hd6* underlying flowering time across a diverse
281 rice accessions (Yano et al. 2016). We constructed haplotype networks of these four genes for
282 the 3,010 diverse cultivated rice genomes from the 3,000 Rice Genomes Project (Wang et al.
283 2018) (**Supplemental Fig. S14; Supplemental Table S9**). From 29 million single nucleotide
284 polymorphisms (SNPs), there were more than one hundred SNPs for each gene (*Hd1*, *Hd2*, *Hd5*,
285 and *Hd6*). These four genes were found to have multiple haplotypes but were primarily separated
286 into Xian/Indica (XI) and Geng/Japonica (GJ) accessions.

287

288 Haplotype analysis identified four major haplotypes for *Hd1*, each with more than one hundred
289 accessions. We aligned these SNPs-defined haplotypes with characterized functional
290 polymorphisms (**Fig. 5A; Supplemental Table S10**). One major haplotype with the largest
291 number of accessions was dominated by XI accession with wild-type allele, while another major
292 haplotype with the second largest number of accessions was dominated by GJ accessions
293 carrying either *c.468_500del33* or *c.833_834del2* allele (**Fig. 5A**). We identified six major
294 haplotypes for *Hd2*. Three haplotypes mainly consisted of XI accessions and two mainly GJ
295 accessions. Wild-type haplotype was only detected in XI accessions. Three functional sites,
296 *c.1515_1522del8*, *M457V*, and *Y704H* were also uncovered in XI accessions, while the majority
297 of GJ accessions carried the *G420D* allele. We found *Hd5* had four major haplotypes, with two
298 of them containing more than 800 accessions. One was found to contain mostly XI accessions
299 with either *L19S* or *c.323delA* allele, while the second haplotype contained mostly GJ accessions
300 with wild-type and *c.222G>T* alleles. Additionally, *Hd6* had four major haplotypes, with 1398
301 and 945 accessions for the first two haplotypes. Out of 1398 accessions shared the same
302 haplotype carrying *c.1809delG*, 57% were XI accessions and 35% were GJ accessions. The
303 second haplotype was mainly shared by XI accessions with the allele of *c.1631delA&c.1809delG*.
304 The number of accessions for *Hd6* wild-type allele was 48 and this small group of accessions
305 was not considered as a major haplotype.

306

307 Geographic origins of the 3,010 accessions were primarily comprised of accessions from East,
308 Southeast Asia and India (**Fig. 5B; Supplemental Fig. S15**). We identified a total of 158
309 haplotype combinations (*Hd1: Hd2: Hd5: Hd6*) by aggregating functional alleles from four genes
310 (**Supplemental Table S11**). Ten combinations with more than 50 accessions were regarded as
311 major haplotypes. Combination of *WT: p.G420D: WT: c.1809delG* dominated in the northern
312 region, while combination of *WT: WT: p.L19S: X* (*X* is designated to any haplotype of *Hd6*)
313 accounted for South Asia. China and India contributed the largest numbers of accessions with

314 different haplotype combinations: *WT: p.G420D: WT: c.1809delG* and *WT: c.1515_1522del8:*
 315 *p.L19S: c.1631delA* in China, and *WT: WT: p.L19S: c.1631delA* and *WT: WT: L19S:*
 316 *c1809delG&c.1631delA* in India. To test the significance of genetic differentiation on the
 317 country-level, we assessed population genetic differentiation based on SNPs within the gene loci
 318 (**Supplemental Table S12**). The G_{st} value (Nei and Chesser 1983) was 0.55 from genetic
 319 differentiation between *indica* and *japonica* (Huang et al. 2012a). We obtained the mean G_{st}
 320 values of all pairwise comparisons among 89 countries, which were 0.43 (*Hd1*), 0.37 (*Hd2*), 0.45
 321 (*Hd5*), 0.41 (*Hd6*), and 0.42 (overall across four genes). These numbers suggested a strong
 322 population differentiation and that these genes were selected for local adaptation.

323
 324 To connect the findings from two rice populations (the bi-parental population and the diverse
 325 accessions), we further classified haplotypes at these genes into two functional classes: *WT* and
 326 *non-WT*. With this designation, we were able to leverage the slope value of reaction norm
 327 obtained from the bi-parental population. In the bi-parental population, parent Koshihikari has
 328 the wild-type alleles for *Hd1*, *Hd2*, and *Hd5*, and the mutant allele for *Hd6* (**Supplemental**
 329 **Table S13**). Accordingly, the slope value for *WT* was from the wild-type allele and for *non-WT*
 330 was from the mutant allele. As a result, the identified 158 major haplotype combinations in
 331 diverse rice genomes were categorized into 16 groups ($2^4 = 16$), each with a unique slope value
 332 obtained from the corresponding haplotype combination in the bi-parental population
 333 (**Supplemental Fig. S11**). From the geographic distribution of haplotypes, we observed that
 334 regions with lower mean annual temperature were dominated by haplotypes sensitive to
 335 temperature changes (absolute slope value ≥ 2), while regions with higher temperature had a
 336 majority of haplotypes less responsive to temperature changes (absolute slope value < 2) (**Fig.**
 337 **5C**). This global distribution suggested that combinations of flowering-time plasticity genes have
 338 contributed to the rice expansion and adaptation to around 18 regions and 89 countries.

339 340 **Multiple levels of reaction norms underlying phenotypic complexity**

341 To encapsulate our understanding of phenotypic complexity, we diagrammed multiple reaction
 342 norms along the temperature gradient using findings from the current study as an example. At the
 343 single-locus level, reaction norms of two homozygous genotypes are represented by two alleles
 344 of a major-effect gene (**Fig. 6A**). Within the range of environmental input, they may show a non-
 345 crossover gene-by-environment interaction like *Hd1*, a crossover interaction like *Hd2*, or not
 346 much interaction like *Hd5* and *Hd6*. These patterns emerged out of sorting by individual locus
 347 agree with the reaction norms of genetic effects. Reaction norms at the multi-locus haplotype
 348 level can be revealed by plotting the reaction norms of allelic combinations of major loci (**Fig.**
 349 **6B**). Compared with single-locus, multi-locus haplotypes account for both additive effects and
 350 interactions among genes, reflecting the combined effect from these loci in relevant pathways
 351 and networks. The haplotype combination from alleles with the higher slopes was most plastic
 352 along the environmental index; conversely, most stable (least responsive) for the haplotype
 353 combination from alleles with the lower slopes. Reaction norms of genotypes observed as
 354 individual organisms involved both major genes and many other background genes on the
 355 genome (**Fig. 6C**).

356
 357 Reaction norm at the genome-wide marker effect level has a similar general pattern, representing
 358 the outcome of a genome-wide approach to partition the observed phenotypic variation, different
 359 from other reaction norms. In our study, this series of reaction norms constitute the systematic

360 view of the interplay between genetics and environment in generating the observed phenotypic
361 variation at different resolution levels (**Fig. 1; Fig. 2; Fig. 4; Fig. 6; Supplemental Fig. S10-**
362 **S12**).

363

364 **Discussion**

365 Uncovering genetic architecture and molecular mechanisms of complex traits is important
366 research in biology, evolution, agriculture, and medical science (Mackay et al. 2009; Marais et al.
367 2013). This current study showcased the benefit of pattern discovery in natural environments to
368 explore the interdependent relationship of genetics and environments behind phenotypic
369 plasticity. Specifically, temperature at the early growth stage was found to differentiate the nine
370 environments in which this rice population was grown, and an explicit environmental index was
371 identified to explain, model, and predict rice flowering time. More importantly, changes in size
372 and direction of genetic effects were systematically revealed with reaction norms along the
373 temperature gradient. Genes known to respond to day length changes were found to respond to
374 temperature in these long-day environments. This can be explained by the interconnected
375 pathways in plants in processing different environmental cues (Blackman 2017; Scheres and van
376 der Putten 2017).

377

378 Unlike the earlier study in sorghum where a single bi-parental population was examined (Li et al.
379 2018), in the current study, we uncovered the patterned geographic distributions of multi-gene
380 haplotypes using the whole-genome sequencing data from a set of diverse rice accessions. By
381 projecting the plasticity parameter value (the slope) obtained from the bi-parental population to
382 the diverse accessions, we revealed that these multi-gene haplotypes with either a higher slope
383 value (sensitive to temperature change) or a lower slope value (less responsible to temperature
384 change) are preferentially distributed in different regions. Further research into the complex
385 haplotype networks of flowering-time genes under broad agroecological conditions may
386 eventually explain the patterns of global rice germplasm adaptation at a finer resolution.

387

388 Transition to flowering, a well-recognized trait of plasticity, is one of the most critical stages in
389 the life cycle of a plant. In this study, the same group of genes were found to be underlying both
390 reaction norm parameters, *i.e.*, intercept and slope, even though their effect sizes varied, similar
391 to the earlier study in sorghum (Li et al. 2018). In both cases, the identified environmental index
392 explained a large proportion of variation in environmental mean. Therefore, it appears that a set
393 of genes from overlapping pathways and networks are underlying phenotypic plasticity, but the
394 exact dynamics may differ depending on different input values of the primary environmental
395 factor(s) differentiating these natural field conditions with respect to flowering time. Distinct
396 genetic architectures for intercept and slope detected in a recent maize study (Kusmec et al.
397 2017), in which environmental mean was used, maybe due to joint effects from multiple
398 environmental indices or high genetic diversity involved.

399

400 Building on earlier works about dynamic gene effects (Marais et al. 2013; Li et al. 2018) and the
401 omnigenic model (Boyle et al. 2017), we proposed a conceptual model to reveal the layers of
402 complexity of a quantitative trait using a set of reaction norms along an environmental index:
403 reaction norms of genetic effects at the single-locus level, reaction norms of genotypes at the
404 single-locus level, reaction norms of genotypes at the multi-locus combination level, reaction
405 norms of genome-wide marker effect continua, and reaction norms of genotypes (observed as

406 individuals). Our findings highlighted the need, as well as the gain in clarity, of quantifying the
407 relevant environmental context when we define and estimate the effects of genes underlying
408 complex traits (Marais et al. 2013). Besides these revealed patterns of genetics and environment
409 interplay, we showed that accurate performance prediction can be achieved through the
410 integrated approaches with genome-wide SNPs and the identified environmental index. Finally,
411 we expect to see further integration of knowledge and approaches in studying the genotype-
412 phenotype relationship from the detailed molecular mechanisms perspective (*e.g.*, gene mapping
413 and cloning, molecular and developmental biology, and genome editing) and the broad genomic
414 and environmental diversity perspective (*e.g.*, sequencing, genome-wide association studies,
415 genomic prediction, high throughput phenotyping, and crop model and physiology).

416
417 Assessing genetic effect along the environmental factors provides a way to optimize the
418 utilization of genetic resources in plant breeding process. Abundant allelic variations have been
419 observed at many loci in rice flowering time. Complementary to genome-wide prediction,
420 quantifying the allelic effects and haplotype effects at multiple loci across different
421 environmental gradients can help breeders fine-tune flowering time in rice cultivars with
422 designed introgression or targeted editing (Zeng et al. 2017; Chen et al. 2019). In addition,
423 resource allocation of testing environments can be optimized to better capture major
424 environmental gradients. Besides flowering time, other agriculturally and economically
425 important traits are also strongly affected by environmental conditions and can be examined
426 using the same approaches. Besides temperature and day length, other quantifiable factors, such
427 as soil properties, including soil water retention and plant available water, can also be examined
428 and potentially factored into constructing the environmental index. Understanding the genetic
429 and environmental mechanisms underlying complex traits helps improve crops to satisfy the
430 demand for food supply for still increasing world population under climate change.

431

432 **Methods**

433 **Genetic population and phenotyping**

434 The genetic mapping population from Koshihikari and Kasalath was developed by the National
435 Institute of Agrobiological Sciences Rice Genome Resource Center, Japan. Phenotype and
436 genotype data were detailed in previous studies (Ma et al. 2002; Onogi et al. 2016) and available
437 at <https://github.com/Onogi/HeadingDatePrediction>. Genotypes and a linkage map of 162
438 restriction fragment length polymorphism markers are available at
439 <https://www.rgrc.dna.affrc.go.jp/ineKKBIL182.html>. All these markers are bi-allelic. This
440 population of 174 backcross inbred lines (BILs) was evaluated in six experimental fields across 3
441 years (nine environments in total): Tsukuba (2007, 2008Early, 2008Late, 2009), Ishikawa (2008),
442 Fukuoka (2008), Ishigaki (2008), Thai Nguyen (2008), and Ha Noi (2008) (**Supplemental Table**
443 **S1**). The abbreviations for these trials are: TS07, TS08E, TS08L, TS09, ISA08, FU08, ISI08,
444 TH08, and HA08. Planting dates for these trials varied from March 31 to June 30. At each site,
445 seeds were pre-germinated in water and planted to seedling trays filled with soil. Seedlings were
446 transplanted at the 3-4 leaf stage. Heading dates were recorded for five plants from the middle of
447 each row and the averaged value was recorded, and we used term flowering time to represent
448 heading date. A randomized complete block design (RCBD) was applied in the field and each
449 environment had two replications and the average value was used for each line. Environmental
450 mean of flowering time was calculated as the average heading date for the whole population at
451 each environment.

452

453 **Identifying the environmental index**

454 Environment data for temperature and day length (based on civil twilight) were retrieved from
455 NOAA (National Oceanic and Atmospheric Administration, <https://www.noaa.gov/weather>) and
456 the Astronomical Applications Department of the U.S. Naval Observatory
457 (<https://www.usno.navy.mil/USNO/astronomical-applications>). Daily temperature (°F) was
458 converted to GDD for rice with the formula: $GDD = [(Maximum\ temperature + Minimum\ temperature)/2] - 50$.
459

460

461 We tested three environmental parameters: temperature (expressed as GDD), day length, and
462 PTT ($GDD \times day\ length$) (**Supplemental Table S6**). From each window during development,
463 mean value of each parameter was calculated first and then its correlation with environmental
464 mean of flowering time was obtained. Each window was from a starting day (*i*) to an end day (*j*),
465 and both were expressed as days after planting. The search was conducted with consecutive
466 starting and ending days and only windows before the trait expression were considered. The
467 parameter-window combination with the highest correlation and reasonable biological
468 interpretation was chosen as the final environmental index.

469

470 **Genetic mapping and flower-time genes**

471 We conducted inclusive composite interval mapping with the software ICIM (Meng et al. 2015).
472 A total of 162 markers were used. QTL mapping with additive and epistasis were conducted for
473 flowering time in individual environments and for QTL by environment interactions using multi-
474 environment trials (Li et al. 2006; Li et al. 2015a) (**Supplemental Methods**).

475

476 Intercept and slope were calculated by regressing phenotypes of each individual onto the
477 environmental index using R (R Development Core Team). For mapping of reaction-norm

478 parameters, intercept and slope were treated as phenotypes to detect QTL with ICIM. The
479 significant thresholds were determined with 1,000 times permutations.

480
481 Functional polymorphisms of four flowering-time genes (*Hd1*, *Hd2*, *Hd5*, and *Hd6*) underlying
482 the detected QTLs for the two parental inbreds (Koshihikari and Kasalath) (**Supplemental Table**
483 **S13**) were tabulated from literatures (Yano et al. 2000; Takahashi et al. 2001; Wei et al. 2010;
484 Koo et al. 2013). From the 3,000 Rice Genomes Project (Wang et al. 2018), we obtained the
485 known or potential functional polymorphisms between two parents in four flowering-time genes
486 (**Supplemental Methods**).

487
488 Additional information about reaction norms at multiple levels is presented in **Supplemental**
489 **Methods**.

490
491 **Geographical distribution of haplotypes of flowering-time genes**

492 Across 3,010 rice accessions, polymorphisms (SNPs and small indels) for four genes (*Hd1*, *Hd2*,
493 *Hd5*, and *Hd6*) were extracted from 3,000 Rice Genomes Project (Wang et al. 2018)
494 (<http://iric.irri.org/resources/3000-genomes-project>). There were 143, 475, 282, and 184 SNPs
495 within the gene regions for *Hd1*, *Hd2*, *Hd5*, and *Hd6*, respectively. After filtering with missing
496 rate and minor allele frequency less than 0.05, the number of high-quality SNPs were 11, 74, 14,
497 and 21 for *Hd1*, *Hd2*, *Hd5*, and *Hd6*, respectively. These high-quality SNPs were used to conduct
498 haplotype determination and analyses by using R package “pegas” (Paradis 2010). The minimum
499 number of shared accessions was set as 100 to select major haplotypes.

500
501 Documented functional sites (small insertions, deletions, and large structural variations) were
502 compiled from literatures charactering *Hd1*, *Hd2*, *Hd5*, and *Hd6* (Yano et al. 2000; Takahashi et
503 al. 2001; Wei et al. 2010; Koo et al. 2013) to annotate the haplotypes constructed by SNPs in
504 “pegas”.

505
506 The global temperature visualized in the geographic map was the mean annual temperature for
507 the years 1970-2000 with R package “raster” and function “getData”. The temperature data were
508 from the database “worldclim”, which collects global interpolated climate data.

509
510 **Population genetic differentiation analysis**

511 To test whether accessions with different haplotype combinations were selected for local
512 adaptation, we grouped the 3,010 accessions into 89 countries. R package “mmod” was used to
513 analyze population genetic differentiation (Winter 2012). We applied function “diff_stats” to
514 calculate three different statistics of differentiation using SNPs within the genes extracted from
515 sequence data. The three statistics are *Hs* (Heterozygosity of sub-populations), *Ht*
516 (Heterozygosity of the total population), and *Nei's Gst* (Nei and Chesser 1983), all of which
517 were estimated for individual genes and four genes together (**Supplemental Table S12**).

518
519 **Joint genomic regression analysis (JGRA) for performance prediction**

520 Performance prediction with JGRA was conducted for three scenarios: predicting the
521 performance of tested genotypes in untested environments; untested genotypes in tested
522 environments; and untested genotypes in untested environments (**Supplemental Methods**).
523 Unlike the traditional joint regression analysis, JGRA involved performance prediction of

524 individuals without performance data through genomics and performance prediction for untested
525 environments through environmental index (Li et al. 2018).

526
527 JGRA through reaction-norm parameter approach obtained intercept and slope by regressing
528 individual's performance on environmental index, and connection of individuals with and
529 without performance data was established with the genome-wide relationship (**Supplemental**
530 **Methods**). JGRA through genome-wide marker effect continuum approach obtained genome-
531 wide marker effects at each environment and these effects were then regressed on environmental
532 index to obtain fitted values for prediction. JGRA is a generic framework, which can be applied
533 for input datasets with sizes ranging from small to large. Both genomic prediction with the
534 genome-wide relationship and genome-wide marker effect estimation use rrBLUP as a default
535 setting, which can be customized to accommodate other methods.

536

537 **Acknowledgements**

538 This work is supported by ISU Plant Sciences Institute and ISU Raymond F. Baker Institute for
539 Plant Breeding.

540

541 **Author contributions**

542 J.Y. and X.L. designed research; T.G., X.L., Q.M., J.W., A.V., A.O., and H.I. performed
543 research; and T.G., X.L., and J.Y. wrote the paper with inputs from all other authors.

544

545 **Conflict of interest statement**

546 The authors declare that there are no competing interests in relation to the work described.

547

548 **Reference**

- 549 Bernardo R, Yu J. 2007. Prospects for genomewide selection for quantitative traits in maize. *Crop Science*
550 **47**: 1082-1090.
- 551 Blackman BK. 2017. Changing responses to changing seasons: Natural variation in the plasticity of
552 flowering time. *Plant physiology* **173**: 16-26.
- 553 Boyle EA, Li Yi, Pritchard JK. 2017. An Expanded View of Complex Traits: From Polygenic to Omnigenic.
554 *Cell* **169**: 1177-1186.
- 555 Chen E, Huang X, Tian Z, Wing RA, Han B. 2019. The Genomics of *Oryza* Species Provides Insights into
556 Rice Domestication and Heterosis. *Annual review of plant biology* **70**: 639-665.
- 557 Eberhart St, Russell W. 1966. Stability parameters for comparing varieties 1. *Crop science* **6**: 36-40.
- 558 Finlay K, Wilkinson G. 1963. The analysis of adaptation in a plant-breeding programme. *Australian*
559 *journal of agricultural research* **14**: 742-754.
- 560 Godfray HC, Beddington JR, Crute IR, Haddad L, Lawrence D, Muir JF, Pretty J, Robinson S, Thomas SM,
561 Toulmin C. 2010. Food security: the challenge of feeding 9 billion people. *Science* **327**: 812-818.
- 562 Hayama R, Yokoi S, Tamaki S, Yano M, Shimamoto K. 2003. Adaptation of photoperiodic control
563 pathways produces short-day flowering in rice. *Nature* **422**: 719-722.
- 564 Hori K, Matsubara K, Yano M. 2016. Genetic control of flowering time in rice: integration of Mendelian
565 genetics and genomics. *Theor Appl Genet* **129**: 2241-2252.
- 566 Huang X, Kurata N, Wang Z-X, Wang A, Zhao Q, Zhao Y, Liu K, Lu H, Li W, Guo Y. 2012a. A map of rice
567 genome variation reveals the origin of cultivated rice. *Nature* **490**: 497.
- 568 Huang X, Yang S, Gong J, Zhao Y, Feng Q, Gong H, Li W, Zhan Q, Cheng B, Xia J et al. 2015. Genomic
569 analysis of hybrid rice varieties reveals numerous superior alleles that contribute to heterosis.
570 *Nature communications* **6**: 6258.
- 571 Huang XH, Zhao Y, Wei XH, Li CY, Wang A, Zhao Q, Li WJ, Guo YL, Deng LW, Zhu CR et al. 2012b.
572 Genome-wide association study of flowering time and grain yield traits in a worldwide collection
573 of rice germplasm. *Nature Genetics* **44**: 32-U53.
- 574 Itoh H, Nonoue Y, Yano M, Izawa T. 2010. A pair of floral regulators sets critical day length for Hd3a
575 florigen expression in rice. *Nat Genet* **42**: 635-638.
- 576 Josephs EB. 2018. Determining the evolutionary forces shaping G x E. *The New phytologist* **219**: 31-36.
- 577 Koo BH, Yoo SC, Park JW, Kwon CT, Lee BD, An G, Zhang ZY, Li JJ, Li ZC, Paek NC. 2013. Natural Variation
578 in OsPRR37 Regulates Heading Date and Contributes to Rice Cultivation at a Wide Range of
579 Latitudes. *Mol Plant* **6**: 1877-1888.
- 580 Kusmec A, Srinivasan S, Nettleton D, Schnable PS. 2017. Distinct genetic architectures for phenotype
581 means and plasticities in *Zea mays*. *Nature plants* **3**: 715.
- 582 Li H, Ye G, Wang J. 2006. A modified algorithm for the improvement of composite interval mapping.
583 *Genetics*.
- 584 Li S, Wang J, Zhang L. 2015a. Inclusive composite interval mapping of QTL by environment interactions in
585 biparental populations. *PLoS One* **10**: e0132414.
- 586 Li X, Guo TT, Mu Q, Li XR, Yu JM. 2018. Genomic and environmental determinants and their interplay
587 underlying phenotypic plasticity. *Proceedings of the National Academy of Sciences of the United*
588 *States of America* **115**: 6679-6684.
- 589 Li X, Liu H, Wang M, Liu H, Tian X, Zhou W, Lu T, Wang Z, Chu C, Fang J et al. 2015b. Combinations of Hd2
590 and Hd4 genes determine rice adaptability to Heilongjiang Province, northern limit of China. *J*
591 *Integr Plant Biol* **57**: 698-707.
- 592 Ma JF, Shen R, Zhao Z, Wissuwa M, Takeuchi Y, Ebitani T, Yano M. 2002. Response of rice to Al stress and
593 identification of quantitative trait loci for Al tolerance. *Plant and Cell Physiology* **43**: 652-659.
- 594 Mackay TF, Stone EA, Ayroles JF. 2009. The genetics of quantitative traits: challenges and prospects. *Nat*
595 *Rev Genet* **10**: 565-577.

- 596 Malosetti M, Ribaut JM, van Eeuwijk FA. 2013. The statistical analysis of multi-environment data:
597 modeling genotype-by-environment interaction and its genetic basis. *Front Physiol* **4**: 44.
- 598 Marais DLD, Hernandez KM, Juenger TE. 2013. Genotype-by-environment interaction and plasticity:
599 Exploring genomic responses of plants to the abiotic environment. *Annual Review of Ecology,*
600 *Evolution, and Systematics* **44**: 5-29.
- 601 Matsubara K, Hori K, Ogiso-Tanaka E, Yano M. 2014. Cloning of quantitative trait genes from rice reveals
602 conservation and divergence of photoperiod flowering pathways in Arabidopsis and rice. *Front*
603 *Plant Sci* **5**: 193.
- 604 McCouch S, Baute GJ, Bradeen J, Bramel P, Bretting PK, Buckler E, Burke JM, Charest D, Cloutier S, Cole G
605 et al. 2013. Agriculture: Feeding the future. *Nature* **499**: 23-24.
- 606 Meng L, Li H, Zhang L, Wang J. 2015. QTL IciMapping: Integrated software for genetic linkage map
607 construction and quantitative trait locus mapping in biparental populations. *The Crop Journal* **3**:
608 269-283.
- 609 Millet EJ, Kruijer W, Coupel-Ledru A, Alvarez Prado S, Cabrera-Bosquet L, Lacube S, Charcosset A,
610 Welcker C, van Eeuwijk F, Tardieu F. 2019. Genomic prediction of maize yield across European
611 environmental conditions. *Nat Genet* **51**: 952-956.
- 612 Nei M, Chesser RK. 1983. Estimation of fixation indices and gene diversities. *Annals of human genetics*
613 **47**: 253-259.
- 614 Nicotra AB, Atkin OK, Bonser SP, Davidson AM, Finnegan EJ, Mathesius U, Poot P, Purugganan MD,
615 Richards CL, Valladares F et al. 2010. Plant phenotypic plasticity in a changing climate. *Trends in*
616 *plant science* **15**: 684-692.
- 617 Nuñez FD, Yamada T. 2017. Molecular regulation of flowering time in grasses. *Agronomy* **7**: 17.
- 618 Onogi A, Watanabe M, Mochizuki T, Hayashi T, Nakagawa H, Hasegawa T, Iwata H. 2016. Toward
619 integration of genomic selection with crop modelling: the development of an integrated
620 approach to predicting rice heading dates. *Theoretical and Applied Genetics* **129**: 805-817.
- 621 Paradis E. 2010. pegas: an R package for population genetics with an integrated–modular approach.
622 *Bioinformatics* **26**: 419-420.
- 623 Scheres B, van der Putten WH. 2017. The plant perceptron connects environment to development.
624 *Nature* **543**: 337-345.
- 625 Shrestha R, Gomez-Ariza J, Brambilla V, Fornara F. 2014. Molecular control of seasonal flowering in rice,
626 arabidopsis and temperate cereals. *Ann Bot-London* **114**: 1445-1458.
- 627 Takahashi Y, Shomura A, Sasaki T, Yano M. 2001. Hd6, a rice quantitative trait locus involved in
628 photoperiod sensitivity, encodes the alpha subunit of protein kinase CK2. *Proceedings of the*
629 *National Academy of Sciences of the United States of America* **98**: 7922-7927.
- 630 Tamaki S, Matsuo S, Wong HL, Yokoi S, Shimamoto K. 2007. Hd3a protein is a mobile flowering signal in
631 rice. *Science* **316**: 1033-1036.
- 632 Vergara BS, Chang TT. 1985. *The flowering response of the rice plant to photoperiod*. IRRI, Los Banos.
- 633 Wang W, Mauleon R, Hu Z, Chebotarov D, Tai S, Wu Z, Li M, Zheng T, Fuentes RR, Zhang F. 2018.
634 Genomic variation in 3,010 diverse accessions of Asian cultivated rice. *Nature* **557**: 43.
- 635 Wei XJ, Xu JF, Guo HN, Jiang L, Chen SH, Yu CY, Zhou ZL, Hu PS, Zhai HQ, Wan JM. 2010. DTH8 Suppresses
636 Flowering in Rice, Influencing Plant Height and Yield Potential Simultaneously. *Plant Physiol* **153**:
637 1747-1758.
- 638 Winter DJ. 2012. MMOD: an R library for the calculation of population differentiation statistics. *Mol Ecol*
639 *Resour* **12**: 1158-1160.
- 640 Xue W, Xing Y, Weng X, Zhao Y, Tang W, Wang L, Zhou H, Yu S, Xu C, Li X et al. 2008a. Natural variation in
641 Ghd7 is an important regulator of heading date and yield potential in rice. *Nat Genet* **40**: 761-
642 767.

643 Xue WY, Xing YZ, Weng XY, Zhao Y, Tang WJ, Wang L, Zhou HJ, Yu SB, Xu CG, Li XH et al. 2008b. Natural
644 variation in Ghd7 is an important regulator of heading date and yield potential in rice. *Nature*
645 *Genetics* **40**: 761-767.

646 Yano K, Yamamoto E, Aya K, Takeuchi H, Lo PC, Hu L, Yamasaki M, Yoshida S, Kitano H, Hirano K et al.
647 2016. Genome-wide association study using whole-genome sequencing rapidly identifies new
648 genes influencing agronomic traits in rice. *Nat Genet* **48**: 927-934.

649 Yano M, Katayose Y, Ashikari M, Yamanouchi U, Monna L, Fuse T, Baba T, Yamamoto K, Umehara Y,
650 Nagamura Y et al. 2000. Hd1, a major photoperiod sensitivity quantitative trait locus in rice, is
651 closely related to the arabidopsis flowering time gene CONSTANS. *Plant Cell* **12**: 2473-2483.

652 Yeang HY. 2013. Solar rhythm in the regulation of photoperiodic flowering of long-day and short-day
653 plants. *J Exp Bot* **64**: 2643-2652.

654 Zeng D, Tian Z, Rao Y, Dong G, Yang Y, Huang L, Leng Y, Xu J, Sun C, Zhang G et al. 2017. Rational design
655 of high-yield and superior-quality rice. *Nat Plants* **3**: 17031.

656 Zhang ZY, Hu W, Shen GJ, Liu HY, Hu Y, Zhou XC, Liu TM, Xing YZ. 2017. Alternative functions of Hd1 in
657 repressing or promoting heading are determined by Ghd7 status under long-day conditions. *Sci*
658 *Rep-Uk* **7**.

659 Zhao K, Tung CW, Eizenga GC, Wright MH, Ali ML, Price AH, Norton GJ, Islam MR, Reynolds A, Mezey J et
660 al. 2011. Genome-wide association mapping reveals a rich genetic architecture of complex traits
661 in *Oryza sativa*. *Nature communications* **2**: 467.

662

663

Figure legends

664
665
666
667
668
669
670
671
672

Fig. 1. Flowering-time plasticity in rice. **(A)** Nine natural field environments. **(B)** Reaction norm for flowering time based on average day length (from planting to 50 DAP). **(C)** Principal component analysis of $G \times E$ from the additive main effect and multiplicative interaction (AMMI) model. **(D)** Reaction norm based on a numerical order of environmental mean. Regression fitted lines are indicated for two parents in panel D. Dots are the observed flowering-time values. DAP, days after planting.

673
674
675
676
677
678
679

Fig. 2. Identifying an environmental index from the performance data. **(A)** Rice development and temperature (in GDD) profiles across different environments. **(B)** Search for the most indicative growth window within which average temperature is highly correlated to environmental mean of flowering time. Temperature within the window of 9-50 days after planting was chosen as the environmental index and denoted as GDD_{9-50} . **(C)** Significant correlation between GDD_{9-50} and environmental mean. **(D)** Regression-fitted reaction norm using environmental index (GDD_{9-50}) as the explanatory variable.

680
681
682
683
684
685
686
687
688

Fig. 3. Performance prediction of flowering time with joint genomic regression analysis (JGRA) to leverage environmental index and genomic prediction. **(A-C)** JGRA using reaction-norm parameters. **(D-F)** JGRA using genome-wide marker effect continua. The three scenarios are: predicting performance for tested genotypes in untested environments (A, D), predicting untested genotypes in tested environments (B, E), and predicting untested genotypes in untested environments (C, F). Prediction accuracy within each individual environment (in parentheses) and across all environments (r) are indicated; the diagonal line indicates the exact match between observed and predicted values.

689
690
691
692
693
694
695
696
697
698
699
700
701
702

Fig. 4. Varied effects at four loci along the temperature gradient underlying the rice flowering-time plasticity. **(A)** Reaction norms of genetic effects at single-locus level along the environmental index by temperature (GDD_{9-50}). Dots show the effects detected from individual environment analysis. Dashed vertical line shows the positions of intercepts at the average temperature value. **(B)** Loci detected by mapping using the parameters (intercept and slope) derived from the reaction norms of genotypes. Horizontal lines in LOD plots show the significance threshold. Additive effect in descending absolute-value order for intercept: *Hd5*, *Hd1*, *Hd6*, and *Hd2*; and for slope: *Hd1*, *Hd2*, *Hd5*, and *Hd6*. **(C)** Known or potential functional polymorphisms between two alleles in four flowering-time genes from sequence analysis. **(D)** Positions of four genes highlighted in the rice flowering control pathway under natural long day-length (LD) conditions. These genes originally discovered for photoperiodic response are found to be involved in sensing temperature differences in LD. Pathway diagram is modified following the figure 1 in (Matsubara et al. 2014).

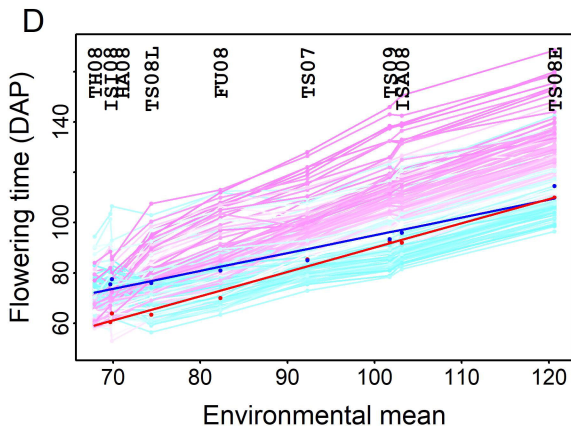
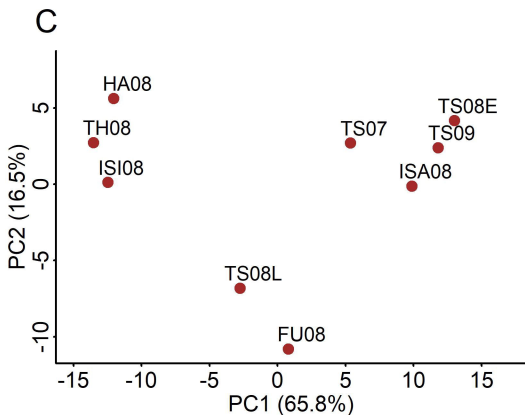
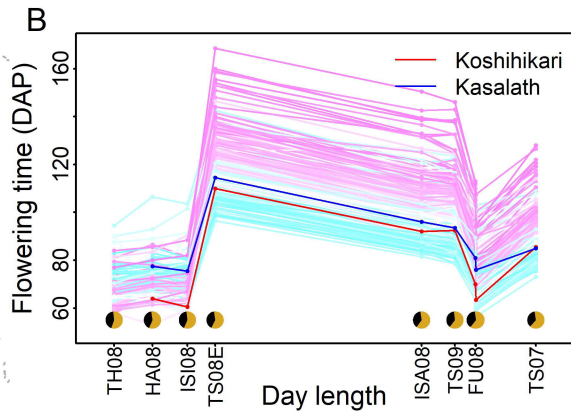
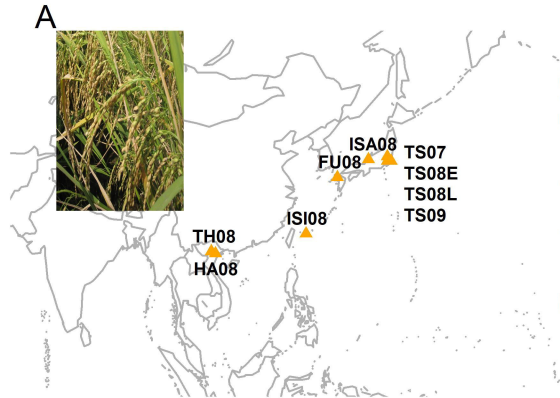
703
704
705
706
707
708
709

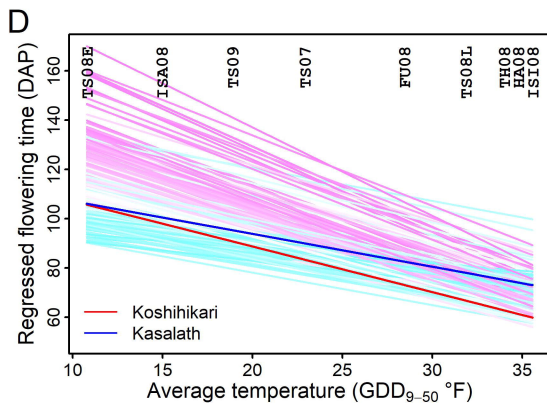
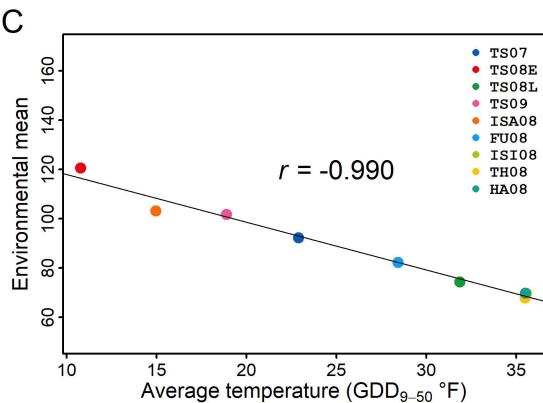
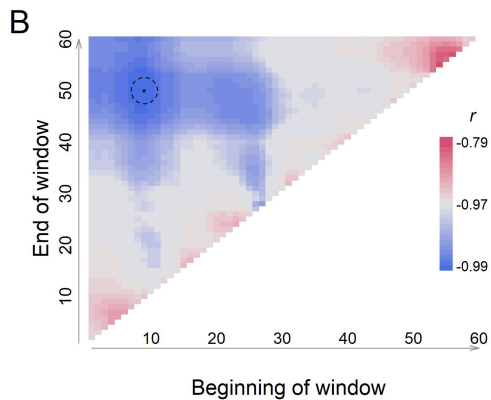
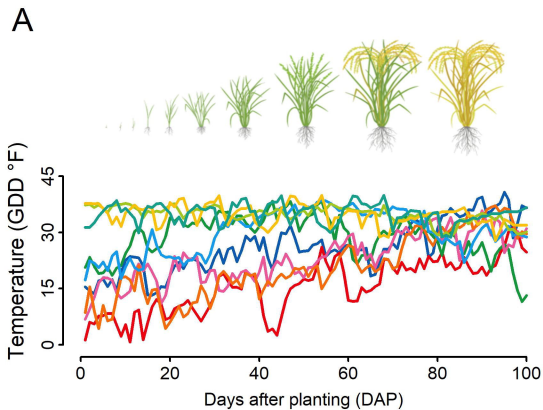
Fig. 5. Natural allelic variations in the *Hd1*, *Hd2*, *Hd5*, and *Hd6* among 3,000 rice genomes materials. **(A)** Haplotype network of four genes from 3,010 rice accessions. Haplotype frequencies are proportional to the sizes of the circles. Each major haplotype is annotated with the functional sites. The total number of accessions used for haplotype analysis vary among 4 genes. The different colors represent the classification of rice accessions. **(B)** Geographic distribution of the four-gene combinations in rice accessions. The different colors represent

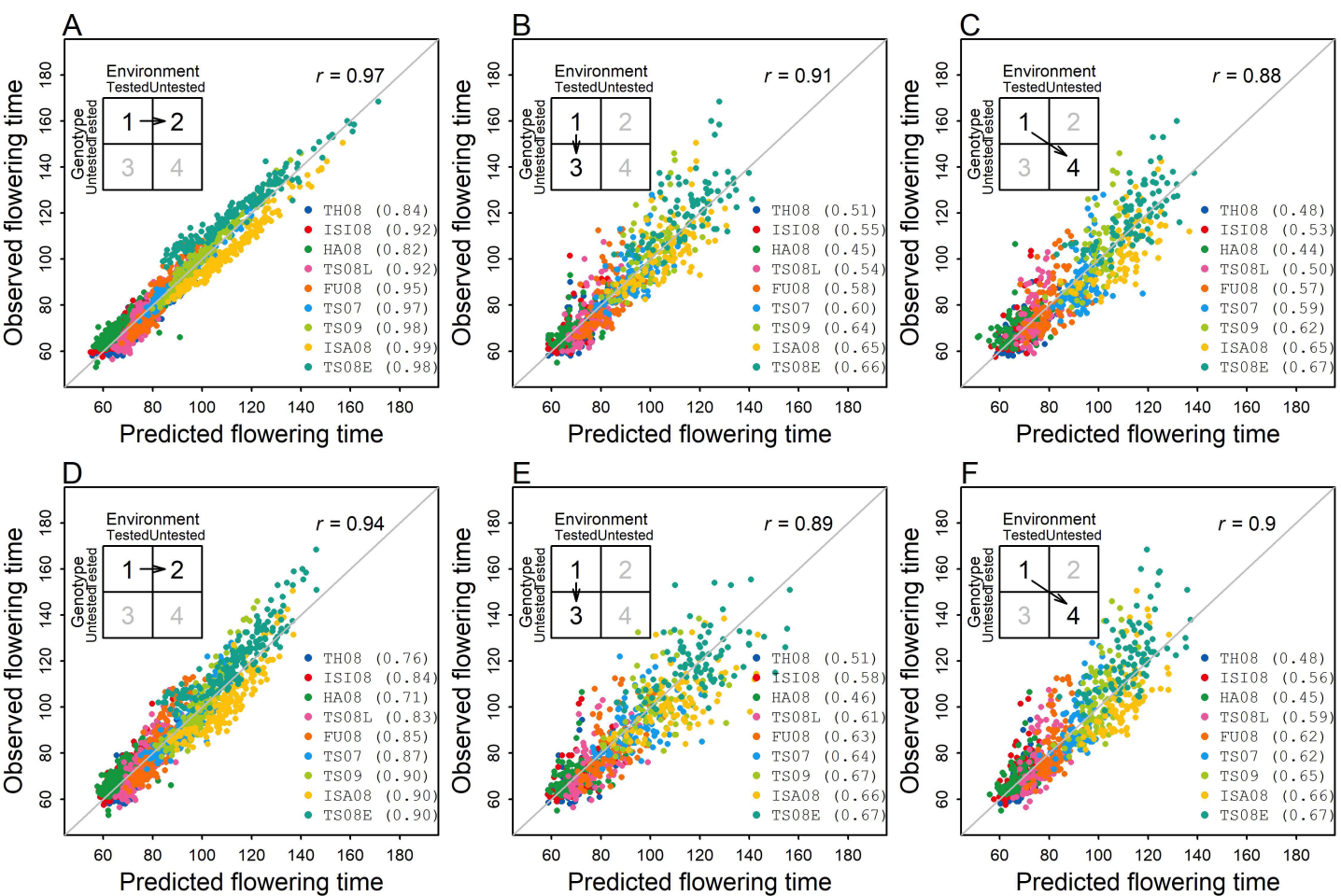
710 different combinations of *Hd1*, *Hd2*, *Hd5*, and *Hd6*. The relative size of each pie indicates the
711 ratio of accessions within each combination in a given country. (C) Geographic distribution of
712 the multi-gene haplotypes with different slope values indicating the sensitivity to temperature.
713 High slope, absolute value ≥ 2 ; low slope, absolute value < 2 .

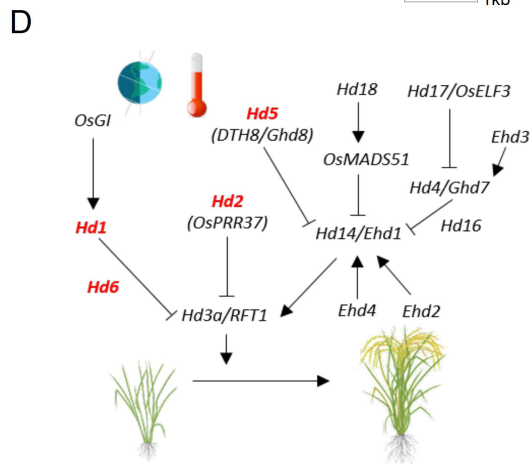
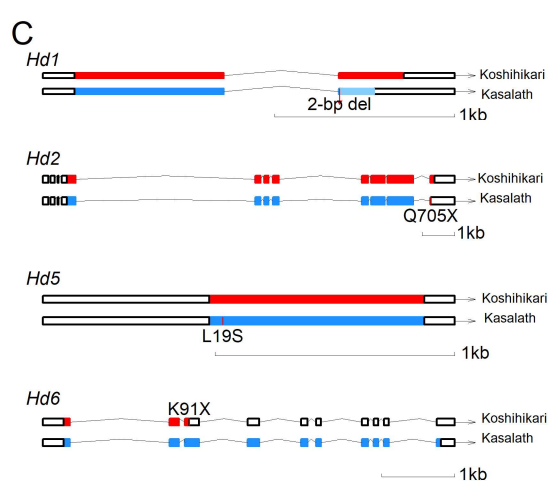
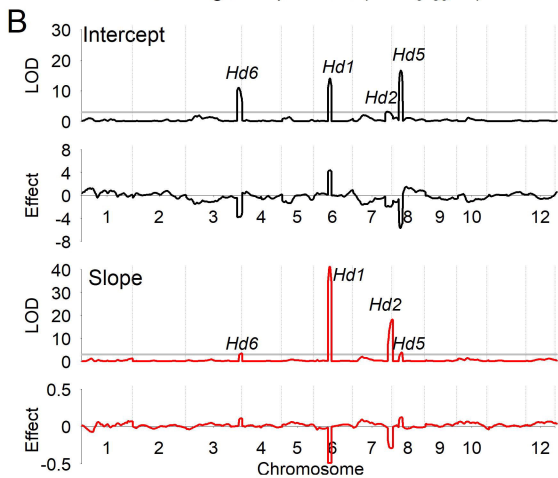
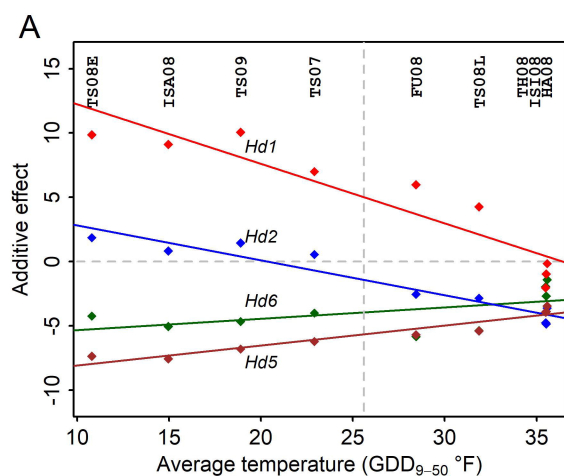
714

715 **Fig. 6.** A conceptual model to explain phenotypic complexity using reaction norms at multiple
716 levels with varied environmental inputs. (A) Reaction norms at the single-locus level to
717 temperature changes. Two homozygous genotype classes are represented by two alleles for the
718 gene *Hd1*. (B) Reaction norms at the multi-locus haplotype level to temperature changes. The
719 $2^4=16$ haplotype (homozygous genotype) classes are shown for four genes (*Hd1*, *Hd2*, *Hd5*, and
720 *Hd6*). (C) Reaction norms at the genome level observed as individual organisms to temperature
721 changes.

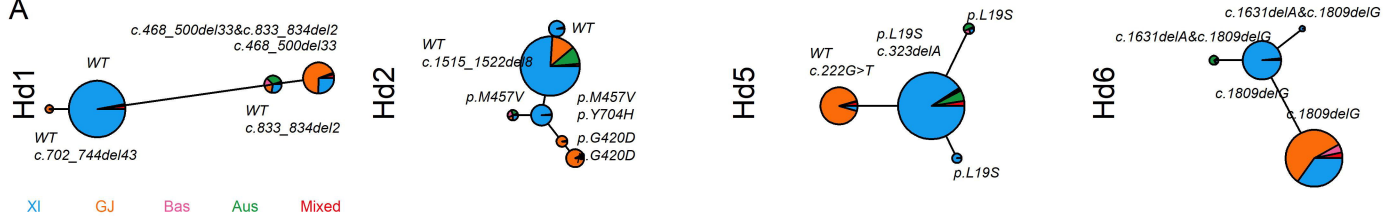




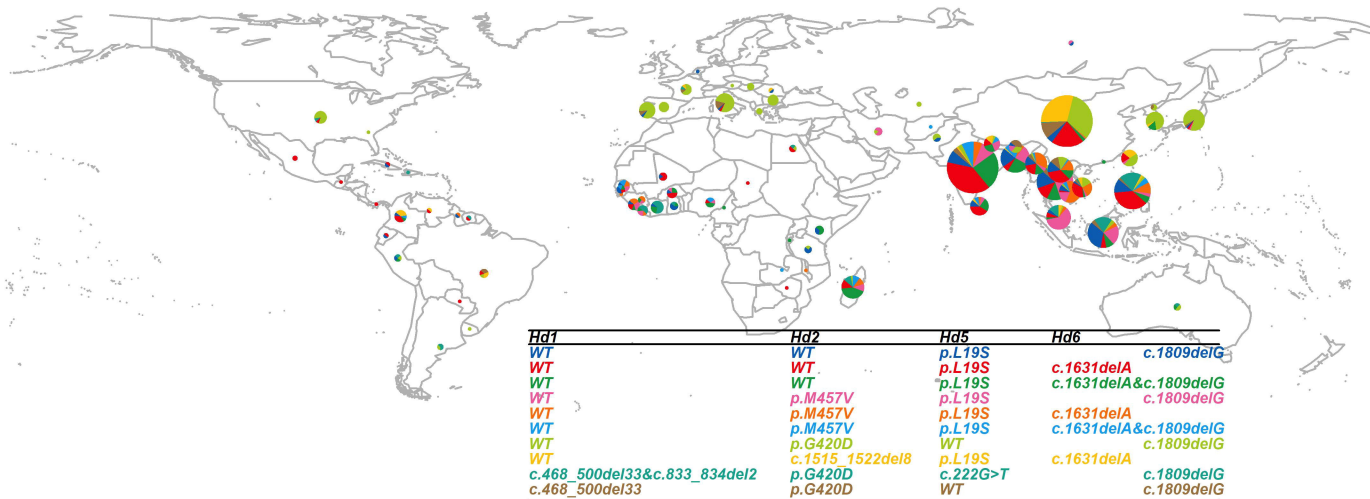




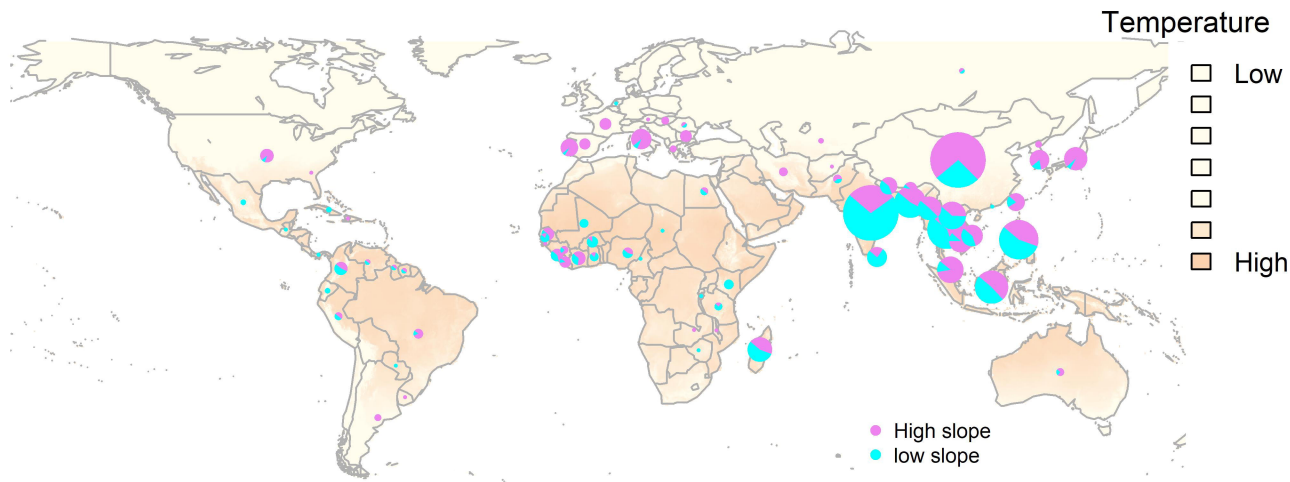
A



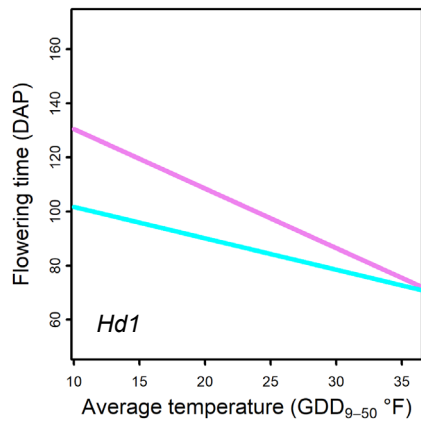
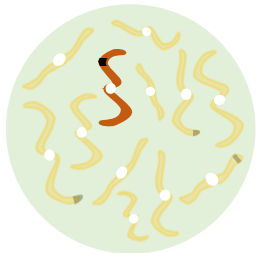
B



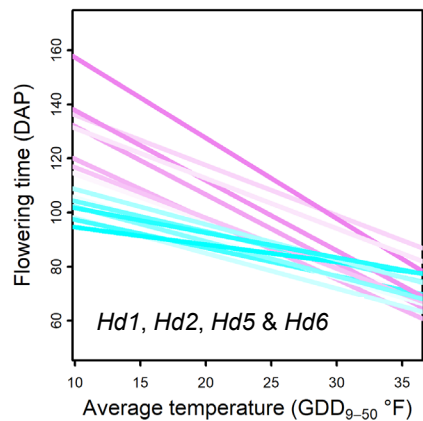
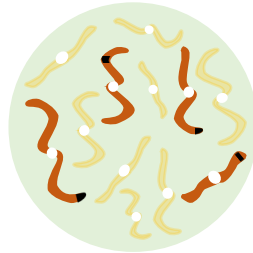
C



A Single Locus



B Multi-locus Haplotype



C Genome

